Monatshefte für Chemie 105, 1344—1361 (1974)

Thermodynamic Properties of Iron—Tellurium Alloys

By

H. Ipser and **K. L. Komarek**

Institute of Inorganic Chemistry, University of Vienna, Austria

With 7 Figures

(Received September 19, 1974)

Vapor pressures of tellurium of iron—tellurium alloys were determined between 550 and 900 °C and between 0 and 67 at% Te by an isopiestic method. Activities and partial molar enthalpies of tellurium were calculated and integral free energies of formation were obtained by a *Gibbs-Duhem* integration. Two statistical models were used to calculate activities in the hexagonal δ′-NiAs phase. Excellent agreement with the experimental values was obtained by assuming random distribution of iron atoms and iron vacancies in the defected (00½) layers of the lattice. The interaction energy between iron vacancies was found to be 820 cal · g-atom^{-1}.

In a series of investigations activities of tellurium in the Ni—Te[1] and Co—Te[2] system and activities of selenium in the Ni—Se[3] and Co—Se[4] system have been studied by an isopiestic method paying special attention to the nonstoichiometric NiAs-type phases in those systems. In the Fe—Te system the NiAs-phase is stable only at elevated temperature which makes the isopiestic method especially suitable for activity measurements.

The phases and boundaries in the Fe—Te phase diagram have been studied and described in another publication[5] incorporating phase boundary information obtained from the isopiestic measurements.

The heat of solution of an alloy with 50 at% Te in bromine water was determined by *Fabre*[6] who calculated from it the enthalpy of formation as — 7.79 kcal/g-atom. *Wagman* et al.[7] reevaluated this result and gave a value of $\Delta H^{\circ}_{f,298} = -7.5$ kcal/g-atom. *Westrum*, *Chou*, and *Grønvold*[8] determined heat capacities of Fe—Te alloys with 47.5 and 66.7 at% Te between 5 and 350 K, and *Mikler* et al.[9] made heat capacity measurements on two alloys of the same composition at higher temperatures. *Rumyantsev* et al.[10] found the dissociation pressure of an alloy with 50 at% Te between 600 and 750 °C to be 0.016 to 0.6 Torr. *Geiderikh* et al.[11] and *Gerasimov*

et al.[12] made *emf* measurements on solid Fe—Te alloys and calculated integral thermodynamic properties. The literature data were critically evaluated by *Mills*[13].

In the present study activities of tellurium were determined by equilibrating iron specimens with tellurium vapor from a reservoir kept at the temperature minimum of an evacuated closed tube which was heated in a temperature gradient. Phase boundaries were obtained from discontinuities in the specimen composition vs. temperature curves.

Experimental Procedure

The materials were 0.2 mm thick iron wire of 99.9% purity (Allied Chemical and Dye Corp., USA) and tellurium lumps of 99.99% and 99.999% purity (ASARCO, New York, USA). The 99.99% tellurium was further purified as previously described[5]. The graphite crucibles were machined from high purity graphite rods (density 1.82 g/cm^3, UT-9, Ultra Carbon Corp., Mich., USA).

The iron wire was wound into little spools of 12 to 15 turns and about 10 mm diameter weighing 100 to 125 mg. These specimens were degreased in CCl_4, thoroughly rinsed with acetone, and dried.

The first two experiments were carried out in an apparatus very similar in design to those employed in previous investigations[1–4]. The only modification was an anular quartz insert in the graphite crucibles to avoid contact between the iron specimens and graphite. The other six experiments were performed in an all-quartz system which is shown in Fig. 1. It consisted of an outer tube (38 mm O.D., 2 mm wall thickness), an inner thermocouple protection tube (7 mm O.D., 1 mm wall thickness) with an enlarged upper part (33 mm O.D.), and a reservoir crucible (33 mm O.D., 70 mm high) with a 500 mm long slit tube (19 mm I.D.) attached. The outer tube had on top a ground joint for a connection with a high vacuum system, and the slit tube contained the specimen crucibles stacked one above the other. Each crucible (18 mm O.D., 23 mm high, 1.5 mm wall thickness) had a ground top and bottom with a small slit so that each crucible served as a cover for the one underneath with an opening of about 0.2 mm between them.

All quartz parts were first cleaned with HNO_3, then with a mixed acid (5% HF, 30% HNO_3, rest dist. H_2O), rinsed with distilled water and dried. The quartz tubes with empty crucibles were evacuated to 10^{-3} torr, heated over night in a furnace at 900 °C and backfilled at 800 °C with purified argon to prevent adsorption of moisture. After cooling to room temperature the reservoir crucible was loaded with about 50 g tellurium. Specimen crucibles and Fe specimens were weighed separately and together on a semi-micro balance to within $\pm$ 0.05 mg. The crucibles with specimens were put into the slit tube and the distance of each specimen from the reservoir crucible measured to within $\pm$ 1 mm. The equilibration tube was assembled, the thermocouple protection tube resting on a wad of quartz wool to prevent cracking during the rapid quench at the end of a run, the assembly connected to the high vacuum system, evacuated, three times flushed with purified argon, and finally sealed at 10^{-4} torr.

The equilibration tube was inserted in a vertical resistance furnace which was at the desired temperature and which had two separately

controlled Kanthal windings. The upper heating zone, extending over 850 mm, was separated from the lower one, which was 190 mm long, by a 60 mm long gap to minimize heat transfer from the hotter upper to the colder lower part. A 100 mm long copper cylinder in the lower zone gave a reservoir temperature constant within $\pm$ 1 °C. The vertical temperature

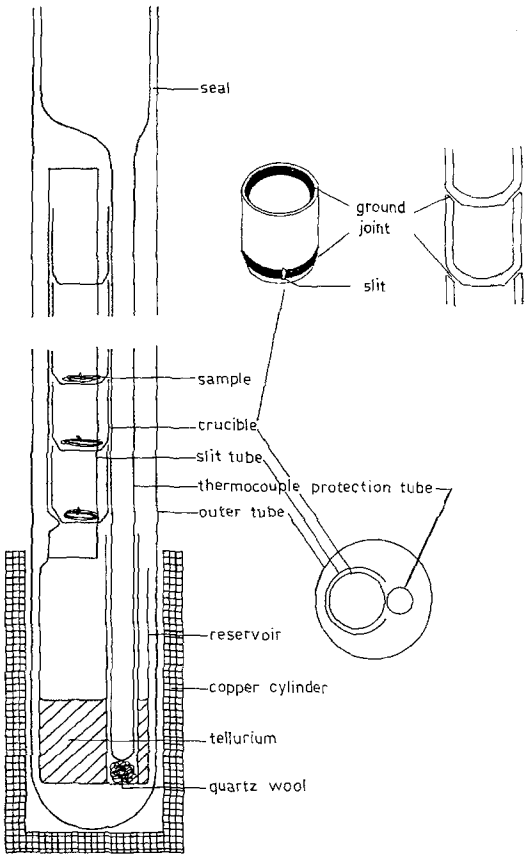

Fig. 1. All-quartz equilibration tube

gradient in the equilibration tube was checked several times during a run by lowering and raising a calibrated Pt/10% Rh-Pt thermocouple in the thermocouple protection tube[3] and the temperatures of the specimens determined within $\pm$ 0.5 °C. In a separate experiment it was established that no horizontal temperature gradients existed within the tube. After several weeks the tube was removed from the furnace and quenched in water. The specimens were reweighed, chemically analyzed, and subjected to X-ray analyses[5].

Experimental Results and Discussion

During the first two runs the specimens were contained in graphite crucibles with quartz inserts and 99.99% tellurium was used as reservoir material. After quenching the equilibrated tubes it was observed that small amounts of iron had been transported via the gas phase from the crucibles at higher temperatures (> 750 °C) to the lower temperature part of the vessel where they deposited on the walls of the tube and the crucibles and reacted with tellurium. This effect made it impossible to calculate the tellurium content of the specimens by weight difference and therefore all samples had to be analyzed. A slight improvement was obtained by eliminating the graphite crucibles and by employing an all-quartz equilibration tube. Only by using semiconductor-grade 99.999% tellurium as reservoir material was it possible to completely suppress the transport reaction. A possible explanation of the phenomenon is the presence of traces of halogen in the 99.99% tellurium which might have formed volatile iron halogenides.

A total of eight runs were carried out, six in the all-quartz equilibration tubes, with reservoir temperatures between 469 and 584 °C and specimen temperatures between 550 and 900 °C. The runs lasted generally from two to four weeks, the only exception being run # 7 which was kept for six weeks in the furnace. Run # 2 was put back after two weeks for another two weeks under identical experimental conditions and no further change of the specimen compositions could be observed. It was therefore concluded that two weeks sufficed to establish equilibrium. An exception concerning specimens in the ε-phase field will be discussed later. The results of the experiments, specimen and reservoir temperatures and specimen compositions, are listed in Table 1. The equilibrium curves, superimposed on the phase diagram[5], are shown in Fig. 2. From the discontinuities of these curves information on phase boundaries was obtained which was used in the construction of the phase diagram[5]. Especially the small two-phase region separating the monoclinically distorted δ- and the hexagonal δ'-NiAs-phase rests mainly on isopiestic evidence. Furthermore, the existence of the high-temperature β'-phase was supported by the unusual shape of the curves of run 1 and 5 and by the trace of the curve of run 2 which differed from those of the other runs in the range 46–49 at% Te. No isopiestic specimens were obtained in the γ-phase region although the existence of γ was clearly established by X-ray measurements[5]. From the position of the equilibrium curves in this range (49–56 at% Te) it can be inferred that the change of the Te activity in the γ-phase field can only be very small and that the γ-phase will be thermodynamically hardly more stable than a $\beta + \delta$ phase mixture.

Table 1. *Experimental Isopiestic Results in the Fe—Te System*

Nr.	T, °C	at% Te	phase	$-\log a_{Te}$	$-\log a_{Te}$ (700 °C)	$-\Delta \bar{H}_{Te}$ kcal · g-atom^{-1}
Run 1			$T_R = 509$ °C		Duration: 24 days	
1	867	46.12	β′	1.196	—	(3.2)
2	859	46.23	β′	1.177	—	(3.0)
3	852	46.42	β′	1.161	—	(2.7)
4	846	46.76	β′	1.147	—	(2.3)
5	837	46.26	β	1.126	1.208	3.0
6	828	46.29	β	1.104	1.179	2.9
7	805	46.29	β	1.046	1.109	2.9
8	789	47.03	β	1.004	1.042	2.0
9	775	47.66	β	0.967	0.986	1.2
10	738	55.99	δ	0.861	—	8.2
11	711	57.42	δ	0.782	0.808	11.0
12	694	58.50	δ	0.729	0.713	12.2
13	668	60.27	δ′	0.644	0.569	9.7
14	654	61.07	δ′	0.596	0.494	9.2
15	636	62.09	δ′	0.532	0.394	8.8
16	626	62.69	δ′	0.496	0.336	8.6
17	607	64.28	δ′	0.424	—	8.2
Run 2			$T_R = 546$ °C		Duration: 14 days	
1	869	47.86	β′	1.029	—	(1.0)
2	863	47.50	β′	1.015	—	(1.4)
3	859	47.53	β′	1.006	—	(1.4)
4	851	47.79	β′	0.987	—	(1.1)
5	834	47.90	β′	0.946	—	(0.9)
6	826	48.20	β′	0.927	—	(0.5)
7	819	48.53	β′	0.909	—	(0.1)
8	802	48.83	β′	0.865	—	(— 0.3)
9	791	55.48	δ	0.838	—	6.9
10	777	56.15	δ	0.800	—	8.5
11	763	56.54	δ	0.762	0.889	9.4
12	734	57.76	δ	0.679	0.766	11.4
13	716	58.77	δ	0.625	0.671	12.4
14	705	59.84	δ′	0.591	0.603	10.2
15	692	60.39	δ′	0.550	0.531	9.6
16	672	61.88	δ′	0.483	0.424	8.8
17	657	62.67	δ′	0.434	0.344	8.6
18	646	63.27	δ′	0.396	0.285	8.5
19	635	64.14	δ′	0.357	—	8.3
20	621	64.57	δ′	0.305	—	8.2
Run 3			$T_R = 562$ °C		Duration: 27 days	
1	852	53.83	L	0.920	—	—
2	838	54.71	L	0.886	—	11.2
3	826	55.39	L	0.856	—	8.3

Table 1 (continued)

Nr.	T, °C	at% Te	phase	$-\log a_{Te}$	$-\log a_{Te}$ (700 °C)	$-\Delta\bar{H}_{Te}$ kcal · g-atom^{-1}
4	807	55.58	δ	0.808	—	7.2
5	788	56.41	δ	0.760	—	9.1
6	765	56.95	δ	0.698	0.839	10.1
7	742	57.90	δ	0.633	0.739	11.6
8	720	59.55	δ′	0.568	0.616	10.5
9	705	60.87	δ′	0.522	0.532	9.3
10	690	61.39	δ′	0.473	0.451	9.0
11	675	62.42	δ′	0.424	0.371	8.7
12	655	63.43	δ′	0.358	—	8.4
13	635	64.13	δ′	0.287	—	8.3
Run 4			T_R = 486 °C		Duration: 26 days	
1	899	0.20	Fe	1.383	—	—
2	878	0.50	Fe	1.337	—	—
3	846	1.30	Fe	1.263	—	—
4	833	40.70	α-Fe + β	1.230	—	—
5	815	46.27	β	1.187	1.256	2.9
6	794	46.43	β	1.133	1.186	2.7
7	768	46.83	β	1.063	1.095	2.2
8	740	47.75	β	0.984	0.994	1.1
9	712	47.99	β	0.901	0.903	0.8
10	682	58.07	δ	0.806	0.757	11.8
11	658	59.55	δ′	0.725	0.619	10.6
12	631	61.77	δ′	0.630	0.479	8.9
13	605	63.26	δ′	0.530	0.323	8.5
Run 5			T_R = 512 °C		Duration: 25 days	
1	843	47.17	β′	1.126	—	(1.8)
2	833	47.11	β′	1.101	—	(1.9)
3	828	47.47	β′	1.089	—	(1.5)
4	820	46.41	β	1.069	1.137	2.8
5	814	46.59	β	1.054	1.113	2.5
6	806	46.73	β	1.034	1.085	2.3
7	797	47.42	β	1.010	1.040	1.5
8	787	47.28	β	0.984	1.016	1.7
9	774	47.82	β	0.950	0.966	1.0
10	760	47.81	β	0.911	0.924	1.0
11	742	56.00	δ	0.860	—	8.2
12	721	57.23	δ	0.798	0.849	10.7
13	701	57.98	δ	0.736	0.739	11.7
14	676	60.13	δ′	0.656	0.600	9.8
15	658	61.15	δ′	0.595	0.504	9.1
16	643	62.12	δ′	0.541	0.417	8.8
17	629	62.88	δ′	0.490	0.337	8.6
18	614	63.75	δ′	0.436	—	8.4

Table 1 (continued)

Nr.	T, °C	at% Te	phase	$-\log a_{Te}$	$-\log a_{Te}$ (700 °C)	$-\Delta\bar{H}_{Te}$ kcal · g-atom^{-1}
Run 6			T_R = 584 °C		Duration: 24 days	
1	832	56.45	L	0.780	—	5.5
2	830	56.63	L	0.774	—	5.1
3	827	56.76	L	0.768	—	4.8
4	824	56.96	L	0.759	—	4.4
5	820	57.16	L	0.751	—	4.0
6	815	57.48	L	0.738	—	3.6
7	810	57.83	L	0.725	—	2.7
8	804	58.13	L	0.710	—	2.2
9	798	56.61	δ	0.695	0.890	9.5
10	791	56.81	δ	0.675	0.863	9.9
11	782	57.20	δ	0.652	0.837	10.6
12	773	57.55	δ	0.628	0.806	11.3
13	764	57.90	δ	0.603	0.763	11.6
14	752	58.40	δ	0.570	0.707	12.1
15	738	59.65	δ′	0.530	0.619	10.5
16	722	60.62	δ′	0.482	0.529	9.4
17	704	61.76	δ′	0.427	0.435	8.9
18	683	62.89	δ′	0.358	0.323	8.6
19	663	63.85	δ′	0.293	—	8.4
20	646	64.66	δ′	0.235	—	8.2
21	636	65.00	δ′	0.199	—	8.1
22	633	67.55	ε	0.188	—	—
23	631	67.62	ε	0.181	—	—
Run 7			T_R = 469 °C		Duration: 42 days	
1	777	45.98	β	1.178	1.232	3.3
2	774	45.95	β	1.170	1.222	3.3
3	771	45.97	β	1.161	1.212	3.3
4	768	46.03	β	1.152	1.199	3.2
5	764	45.95	β	1.142	1.188	3.3
6	759	46.15	β	1.128	1.168	3.1
7	753	46.50	β	1.111	1.142	2.7
8	747	46.54	β	1.093	1.120	2.6
9	738	46.83	β	1.068	1.087	2.2
10	728	47.07	β	1.037	1.049	2.0
11	714	47.34	β	0.997	1.001	1.6
12	698	47.68	β	0.947	0.946	1.2
13	682	52.65	β + γ + δ	0.895	—	—
14	659	58.35	δ	0.818	0.700	12.1
15	635	60.04	δ′	0.734	0.574	9.9
16	611	61.57	δ′	0.643	0.441	8.9
17	587	63.26	δ′	0.551	0.301	8.5
18	570	63.54	δ′	0.481	—	8.4

Table 1 (continued)

Nr.	T, °C	at% Te	phase	$-\log a_{Te}$	$-\log a_{Te}$ (700 °C)	$-\Delta \bar{H}_{Te}$ kcal · g-atom^{-1}
Run 8			T_R = 568 °C		Duration: 25 days	
1	843	54.82	L	0.873	—	10.6
2	841	54.97	L	0.868	—	9.9
3	837	55.16	L	0.858	—	9.1
4	835	55.43	L	0.852	—	8.2
5	831	55.57	L	0.843	—	7.7
6	825	55.81	L	0.829	—	7.0
7	820	56.08	L	0.817	—	6.4
8	814	56.44	L	0.800	—	5.5
9	807	55.79	δ	0.784	—	7.7
10	799	56.09	δ	0.763	—	8.4
11	790	56.35	δ	0.740	—	8.9
12	780	56.81	δ	0.712	0.880	9.9
13	769	57.21	δ	0.682	0.837	10.6
14	755	57.69	δ	0.644	0.780	11.3
15	740	58.35	δ	0.601	0.707	12.1
16	723	59.98	δ'	0.550	0.600	10.0
17	701	61.21	δ'	0.482	0.482	9.1
18	678	62.61	δ'	0.408	0.363	8.6
19	653	64.00	δ'	0.325	—	8.4
20	630	65.00	δ'	0.243	—	8.1

All specimens were one-phase, with the exception of specimen # 4 in run 4 and specimen # 13 in run 7. These two specimens were two-phase, and the upper part of the specimens (at higher temperature) consisted of the phase with less tellurium and the lower part (at lower temperature) turned out to be the neighboring phase with the higher tellurium content. The reason was that the two iron spools were not flat in the crucible and the specimens were very close to the temperature of the tie-line. Of particular interest was specimen # 13 run 7 at 682 °C with the upper half being β-phase and the lower half δ-phase. Careful X-ray analysis of the boundary region between the two phases revealed a thin layer of the γ-phase, in agreement with the phase diagram[5] and with the previous conclusion that the change of the Te activity across the γ-phase field is very small.

Generally, as was pointed out previously, equilibration of the specimens was achieved within two weeks. The only exceptions were those specimens which according to the experimental conditions were supposed to be in the ε-phase field. Instead, the compositions of these samples remained in the δ′-phase field close to the δ′/(δ′ + ε) phase

boundary so that samples close to the reservoir would show again a decrease in Te-concentration. This behavior points to a very slow reaction step in the formation of ε from δ', be it the nucleation of ε and/or the diffusion of Te in ε. Similar problems were encountered with

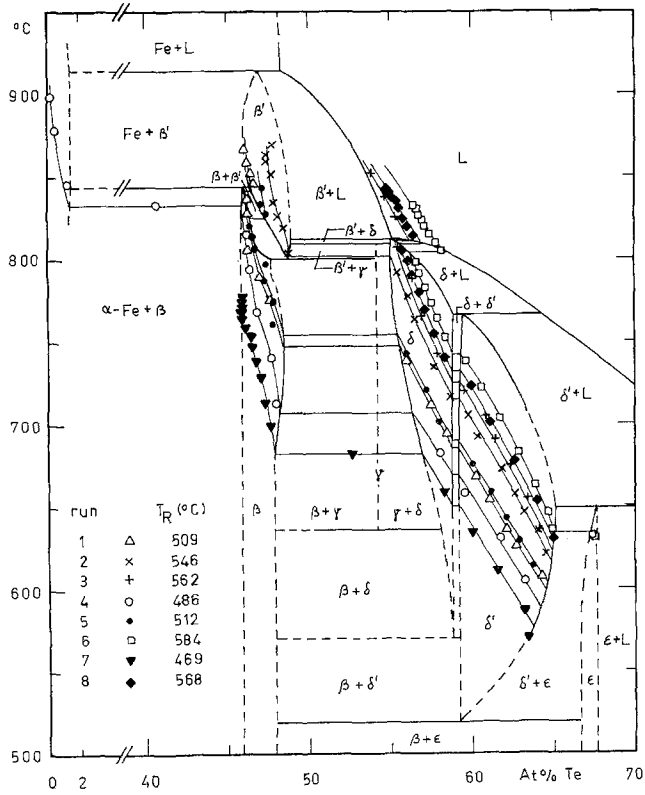

Fig. 2. Specimen composition versus specimen temperature and partial Fe—Te phase diagram

the C18-type phase $CoTe_2$[2] and the C2-type phase $CoSe_2$[4] which required 5 to 8 weeks for equilibration while the C2-type phase $NiSe_2$[3] behaved normally. Run 7 was therefore equilibrated for six weeks but not even such a long period sufficed to obtain specimens in the ε-phase field. Only by first keeping the specimen temperatures so low that the specimens absorbed enough Te to be in the Te-rich liquid phase, and then raising the temperature so that final equilibration occurred by loss of Te from the specimens, was it possible to obtain samples in the ε-phase (specimens # 22 and # 23 in run 6). Specimens which had not attained

equilibrium did not affect equilibration of the other samples in the experiment and were not considered in the subsequent calculations.

In an isopiestic experiment the total vapor pressure in the equilibration tube is determined by the temperature of the pure volatile

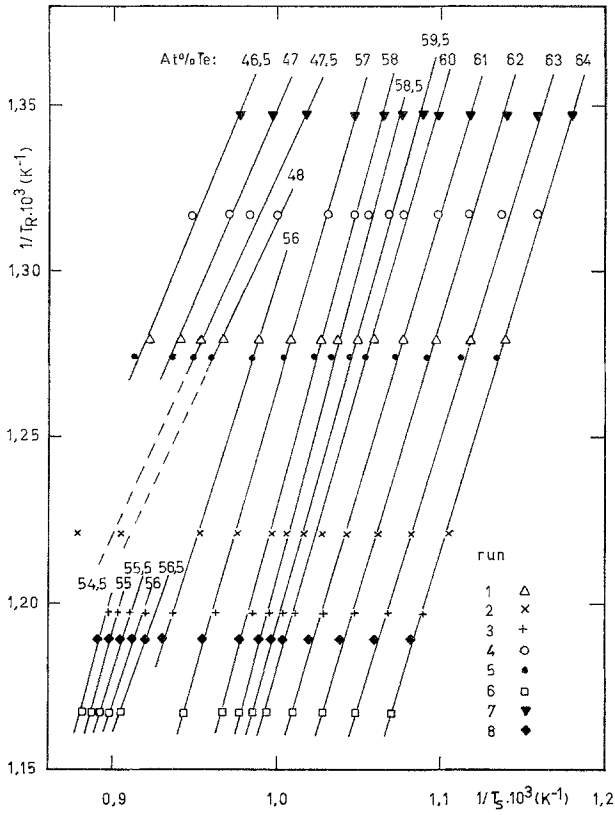

Fig. 3. Reciprocal reservoir temperature versus reciprocal specimen temperature

metal of the reservoir at the temperature minimum. In equilibrium the total sum of the partial pressures of the various species in the gas phase above a specimen is equal to the total vapor pressure in the tube. If the gas phase consists of only one molecular species, as it is the case with tellurium under our experimental conditions with only Te_2 present in significant amounts, the activity can be easily calculated[2] according to

$$a_{Te} = (p_{Te_2}/p^{\circ}_{Te_2})^{1/2} = (p^{\circ}_{Te_2}\,\text{Reservoir Temp.}/p^{\circ}_{Te_2}\,\text{Specimen Temp.})^{1/2} \quad (1)$$

Reciprocal specimen temperatures (T_S), interpolated at fixed temperatures from Fig. 2, are plotted in Fig. 3 as a function of the reciprocal reservoir temperatures (T_R). As can be seen data points of equal composition fall on straight lines which is not only a proof of the consistency of the various runs but can be also used to calculate the partial molar enthalpies of tellurium, $\Delta \bar{H}_{\mathrm{Te}}$ (Fig. 4), employing a form of the *Clausius-*

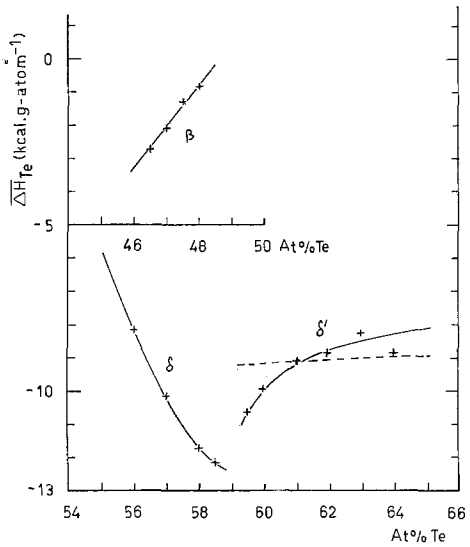

Fig. 4. Partial molar enthalpies of tellurium. + = experimental data; – – – – = calculated data

Clapeyron equation[2]. The data necessary for the calculations, the total vapor pressure and the enthalpy of vaporization of tellurium, were taken from the literature[14]. Activities of tellurium, calculated for each specimen temperature and corrected with the $\Delta \bar{H}_{\mathrm{Te}}$-values for 700 °C, together with the $\Delta \bar{H}_{\mathrm{Te}}$ data are also listed in Table 1. The activity data at 700 °C have been plotted as a function of composition in Fig. 5 and a curve of best fit has been drawn through the data points. Also shown, but without data points, is the activity of tellurium at 825 °C. No $\Delta \bar{H}_{\mathrm{Te}}$ values could be derived for the β′-phase, so the partial molar enthalpies of the β-phase were used to calculate the activities in the β′-phase for 825 °C. The corrections are slight and any error is small since the experimental points for the β′-phase lie between 800° and 870 °C. By assuming at 700 °C a solid solubility of Te in α-Fe of 0.5 at% Te and the position of the α-Fe + β/β phase boundary at

45.9 at% Te and by neglecting the small but unknown change of activity in the γ-phase activities of Fe were obtained by a *Gibbs-Duhem* integration and integral free energies were calculated. The activities

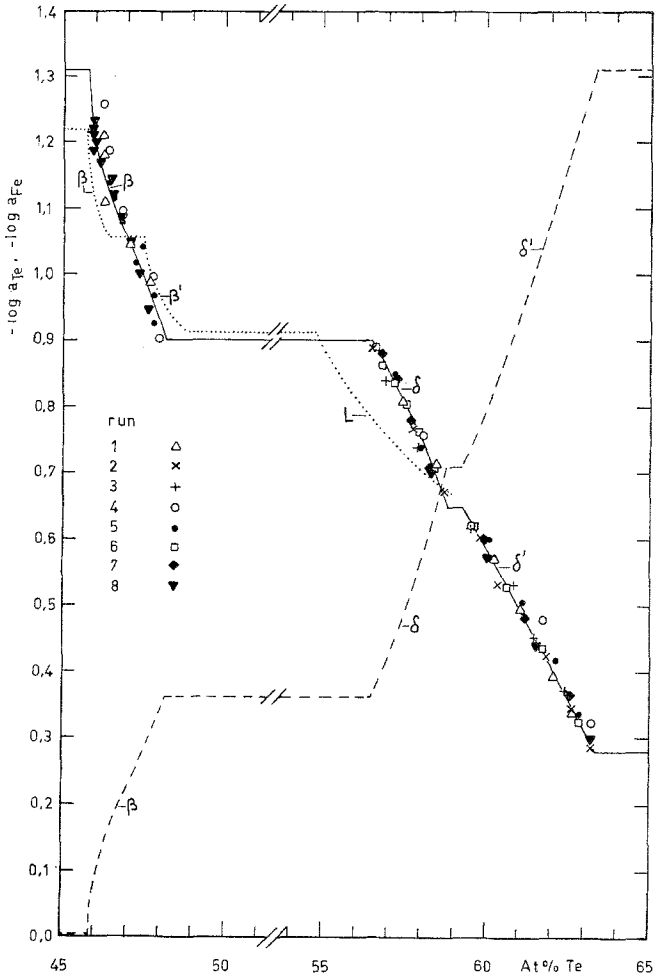

Fig. 5. Activities of tellurium and iron in the iron—tellurium system. ——— = —log a_{Te} (700 °C) with experimental data points; . . . . = —log a_{Te} (825 °C); – – – – = —log a_{Fe} (700 °C)

of Fe are also plotted in Fig. 5. Experimental and calculated values at 700 °C taken from smoothed curves at certain compositions with solid Fe and liquid Te as standard states are listed in Table 2. For some liquid alloys in the range from 54.5 to 56.6 at% Te $\Delta \bar{H}_{Te}$-values have

also been evaluated but their accuracy is certainly less than that of the data for the solid alloys. Those values, given in kcal · g-atom^{-1}, are — 11.5 at 54.5 at% Te, — 11.7 at 55.0 at% Te, — 7.7 at 55.5 at% Te, — 6.6 at 56.0 at% Te, and — 5.3 at 56.5 at% Te.

Table 2. *Thermodynamic Properties of Iron—Tellurium Alloys [Standard states* $Fe_{(s)}$ *and* $Te_{(l)}$*]*

at% Te	phase	$-\log a_{Te}$ (700 °C)	$-\log a_{Fe}$ (700 °C)	$-\Delta G_{700\,°C}$ kcal · · g-atom^{-1}	$-\Delta \bar{H}_{Te}$ kcal · · g-atom^{-1}	$\Delta \bar{S}_{Te}$ cal · · g-atom^{-1} · · K^{-1}
0	α-Fe	∞	0	0	—	—
0.5	α-Fe/(α-Fe + β)	1.310	0.002	0.04	—	—
10.0	α-Fe + β	1.310	0.002	0.59	—	—
20.0	α-Fe + β	1.310	0.002	1.17	—	—
30.0	α-Fe + β	1.310	0.002	1.75	—	—
40.0	α-Fe + β	1.310	0.002	2.34	—	—
45.9	(α-Fe + β)/β	1.310	0.002	2.68	3.4	2.5
46.0	β	1.222	0.073	2.68	3.3	2.2
46.5	β	1.119	0.164	2.71	2.6	2.4
47.0	β	1.051	0.222	2.73	2.0	2.7
47.5	β	0.991	0.275	2.74	1.4	3.1
48.0	β	0.927	0.337	2.76	0.8	3.4
48.2	β/(β + γ)	0.900	0.361	2.76	0.6	3.5
50.0	β + γ	0.900	0.361	2.81	—	—
55.0	γ + δ	0.900	0.361	2.93	—	—
56.5	(γ + δ)/δ	0.900	0.361	2.96	9.2	— 5.4
57.0	δ	0.856	0.418	2.97	10.2	— 6.6
58.0	δ	0.751	0.561	2.99	11.7	— 8.6
58.8	δ/(δ + δ′)	0.648	0.708	2.99	12.4	— 9.8
59.3	(δ + δ′)/δ′	0.648	0.708	2.99	11.0	— 8.4
59.5	δ′	0.627	0.735	2.99	10.7	— 8.1
60.0	δ′	0.585	0.796	2.99	10.0	— 7.6
61.0	δ′	0.498	0.928	2.97	9.2	— 7.2
62.0	δ′	0.409	1.076	2.95	8.8	— 7.2
63.0	δ′	0.312	1.237	2.91	8.5	— 7.3
63.4	δ′/(δ′ + *L*)	0.270	1.310	2.89	8.4	— 7.4
64.0	δ′ + *L*	0.270	1.310	2.87	—	—
70.0	δ′ + *L*	0.270	1.310	2.59	—	—
72.6	(δ′ + *L*)/*L*	0.270	1.310	2.57	—	—

The results can be compared with the data in the literature[10, 11] using heat capacities for the β- and ε-phase[8, 9] and critically compiled entropy and enthalpy values for pure iron and tellurium[16]. For the β-phase (47.3 at% Te) the free energy of formation ΔG (973 K) = = — 2,730 cal · g-atom^{-1} can be combined with the calorimetrically

obtained entropy of formation[9] ΔS (973 K) = — 2.33 cal · K^{-1} g-atom^{-1} to give the enthalpy of formation ΔH (973 K) = —5,000 cal · g-atom^{-1}. *Geiderikh* et al.[11] reported for the β-phase ΔH (700 K) = — 2,650 cal · · g-atom^{-1} and ΔH (800 K) = — 1,750 cal · g-atom^{-1} with solid Te as the standard state at both temperatures. Corrected for the change in standard state and in temperature the first value becomes ΔH (973 K) = = — 5,010 cal · g-atom^{-1}, the second ΔH (973 K) = — 4,000 cal · g-atom^{-1}. Taking ΔH (973 K) = — 5,000 cal · g-atom^{-1} as more reliable the following values have been obtained for the formation of the β-phase from the pure solid components at 298.15 K: ΔH = — 2,500 cal · g-atom^{-1}, ΔS = + 1.04 cal · K^{-1} · g-atom^{-1}, ΔG = — 2,800 cal · g-atom^{-1}.

At 922 K, the peritectic decomposition temperature of the ε-phase (67.6 at% Te), ΔG = — 2,715 cal · g-atom^{-1}. With ΔS (922 K) = = — 5.71 cal · K^{-1}[9] we get ΔH (922 K) = — 7,980 cal · g-atom^{-1}. Referred to solid Te *Geiderikh* et al.[11] found ΔH (700 K) = — 5,420 cal · g-atom^{-1} and ΔH (800 K) = — 5,400 cal · g-atom^{-1}. Referred to liquid Te at 922 K we get ΔH = — 7,980 cal · g-atom^{-1} and ΔH = = — 8,075 cal · g-atom^{-1}, resp. Choosing ΔH (922 K) = — 7,980 cal · g-atom^{-1} the data for the formation of the ε-phase from the pure solid components at 298.15 K are ΔH = — 5,395 cal · g-atom^{-1}, ΔS = = — 2.13 cal · K^{-1} · g-atom^{-1} and ΔG = — 4,760 cal · g-atom^{-1}.

Rumyantsev et al.[10] determined vapor pressures of an Fe—Te alloy with 50 at% Te. From their data one can calculate a_{Te} (600 °C) = = 0.0028 and a_{Te} (700 °C) = 0.0067 which can be compared with our data for an alloy of the same composition, i.e. a_{Te} (600 °C) = 0.120 and a_{Te} (700 °C) = 0.126. Since our data are in good agreement with the phase diagram[5] and with the results of *Geiderikh* et al.[11], the vapor pressures of *Rumyantsev* et al.[10] are apparently too low.

In previous publications[1–4] a statistical model was applied to the defected hexagonal NiAs-structure to derive equations for the calculation of thermodynamic properties. It was assumed that the cation vacancies are confined to *every other* metal atom layer and that cations and cation vacancies in these (00½) layers of the lattice are randomly distributed with interaction energy E_i between the vacancies. The following equations have been derived for this model (model I):

$$\ln a_{Fe} = \ln\left(\frac{1 - 1.5\,N_{Te}}{2\,N_{Te} - 1}\right) - \frac{4\,E_i}{RT}\left(\frac{2\,N_{Te} - 1}{N_{Te}}\right) - \ln K - \frac{E_v}{RT} \qquad (2)$$

$$\ln a_{Te} = \ln\left\{\frac{(N_{Te} - 0.5)}{[N_{Te}\,(0.666 - N_{Te})]^{1/2}}\right\} + \frac{2\,E_i}{RT}\left(\frac{2\,N_{Te} - 1}{N_{Te}^2}\right) + \text{const} \qquad (3)$$

$$\Delta \bar{H}_{\mathrm{Te}} = 2\, E_i \left(\frac{2\, N_{\mathrm{Te}} - 1}{N_{\mathrm{Te}}^2} \right) + \text{const} \tag{4}$$

$$\Delta \bar{S}_{\mathrm{Te}} = -R \ln \left\{ \frac{(N_{\mathrm{Te}} - 0.5)}{[N_{\mathrm{Te}}\,(0.666 - N_{\mathrm{Te}})]^{1/2}} \right\} + \text{const} \tag{5}$$

E_v is the energy of formation of a vacancy and K is the term for non-configurational contributions. In their X-ray investigation of the iron—tellurium system *Grønvold*, *Haraldsen*, and *Vihovde*[15] surmised from intensity measurements of the diffraction lines that the iron vacancies are randomly distributed over *all* metal atom layers of the NiAs-structure. Based on this assumption another set of equations for the activities was derived (model II):

$$\ln a_{\mathrm{Fe}} = \ln \left(\frac{1 - N_{\mathrm{Te}}}{2N_{\mathrm{Te}} - 1} \right) - \frac{2E_i}{RT} \left(\frac{2N_{\mathrm{Te}} - 1}{N_{\mathrm{Te}}} \right) - \ln K - \frac{E_{\mathrm{v}}}{RT} \tag{6}$$

$$\ln a_{\mathrm{Te}} = \ln \left(\frac{N_{\mathrm{Te}} - 0.5}{N_{\mathrm{Te}}} \right) + \frac{E_i}{RT} \left(\frac{2N_{\mathrm{Te}} - 1}{N_{\mathrm{Te}}^2} \right) + \text{const} \tag{7}$$

The interaction energy E_i for both models was obtained by plotting $\log \{a_{\mathrm{Te}}(\mathrm{exp.})[N_{\mathrm{Te}}(0.666 - N_{\mathrm{Te}})]^{1/2}/(N_{\mathrm{Te}} - 0.5)\}$ for model I and $\log \{a_{\mathrm{Te}}(\mathrm{exp.})N_{\mathrm{Te}}/(N_{\mathrm{Te}} - 0.5)\}$ for model II, resp., versus $(2\,N_{\mathrm{Te}} - 1)/N_{\mathrm{Te}}$ (Fig. 6).

At 700 °C the monoclinically distorted δ-phase is stable between 56.3 and 58.8 at% Te and the hexagonal δ′-phase between 59.3 and 63.6 at% Te[5]. As can be seen in Fig. 6 the points in the stability range of the hexagonal δ′-phase fall for both models on straight lines but the line for model II exhibits a break at about 61.7 at% Te. From the slopes of these curves the following interaction energies have been obtained: for model I, $E_i = 820 \pm 20$ cal · g-atom^{-1}, for model II $E_i = 6{,}200 \pm 500$ cal · g-atom^{-1} (between 59.3 and 61.7 at% Te) and $E_i = 10{,}500 \pm 800$ cal · g-atom^{-1} (between 61.7 and 63.6 at% Te). With the interaction energies $E_i = 820$ cal · g-atom^{-1} and $E_i = 6{,}200$ cal · g-atom^{-1}, resp., activities of tellurium were calculated from Eq. (3) and Eq. (7), resp., using in both cases the experimental activity at 59.5 at% Te to determine the constants. The calculated activities are compared with the experimental data at 700 °C in Fig. 7. Also shown in this figure are the activity curves calculated without interaction energies, i.e. omitting the terms containing E_i in Eq. (3) and Eq. (7), resp. Activities from model I with interaction energy are in excellent agreement with the experimental values in the δ′-phase and are even in close accord with the data for the δ-phase at lower tellurium concentrations. The

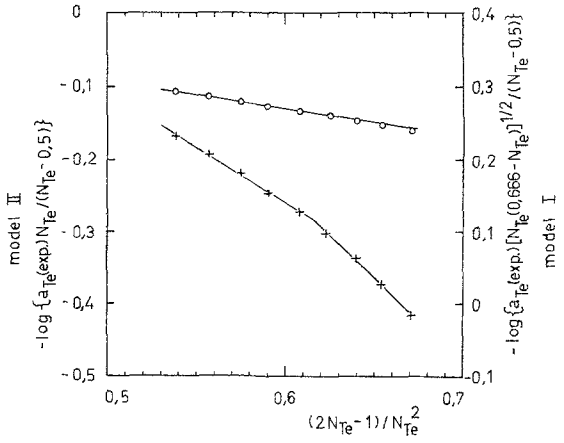

Fig. 6. Diagram for the determination of the interaction energy. O = model I; + = model II

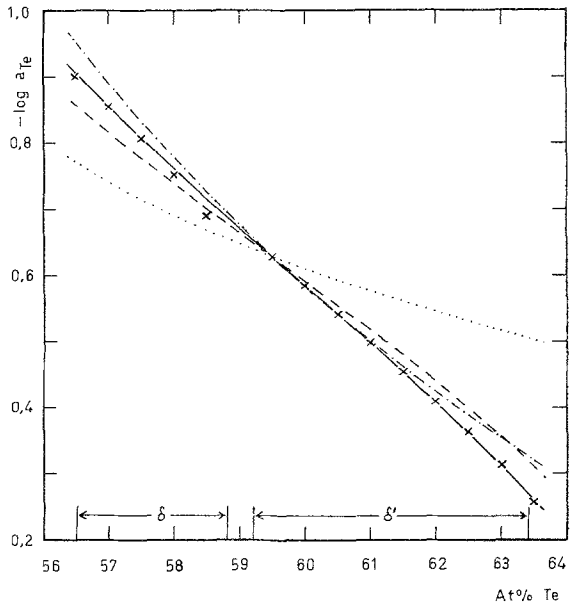

Fig. 7. Calculated and experimental activities of tellurium at 700 °C. × = experimental values; _____ = calculated values [model I-Eq. (3)]; – – – – = calculated values (model I-without interaction energy); –·–·–· = = calculated values [model II-Eq. (7)]; . . . . . = calculated values (model II-without interaction energy)

agreement between activities obtained from model II and the experimental values becomes noticeably poorer with increasing tellurium concentration. This divergence beginning at 61.5 at% Te is apparently also the cause of the break in the curve in Fig. 6. The excellent fit for model I can be considered strong evidence that the cation vacancies in the NiAs-phase of the Fe—Te system are present only in every other metal atom layer of the lattice as is also the case in the Ni—Te[1] and Co—Te[2] system.

The model affords also a test of the partial molar enthalpies. Solving Eq. (4) with $E_i = 820\,\text{cal}\cdot\text{g-atom}^{-1}$ and $\Delta\bar{H}_{\text{Te}}$ (exp.) $= -9{,}100\,\text{cal}\cdot\text{g-atom}$ at 61.0 at% Te we get const $= -10{,}070$ and from it the $\Delta\bar{H}_{\text{Te}}$ (calc.) in Fig. 4. The agreement with $\Delta\bar{H}_{\text{Te}}$ (exp.) is generally good at higher Te concentration but at lower Te content the change of $\Delta\bar{H}_{\text{Te}}$ (exp.) with composition is more pronounced. Since the $\Delta\bar{S}_{\text{Te}}$ (exp.) data are very sensitive to small errors in $\Delta\bar{H}_{\text{Te}}$ (exp.), larger deviations between calculated and experimental values can be expected.

Acknowledgment

The financial support of this investigation by the "Fonds zur Förderung der wissenschaftlichen Forschung" under grant number 1322 is gratefully acknowledged.

References

[1] *M. Ettenberg, K. L. Komarek*, and *E. Miller*, J. Solid State Chem. **1**, 583 (1970).
[2] *R. M. Geffken, K. L. Komarek*, and *E. Miller*, J. Solid State Chem. **4**, 153 (1972).
[3] *H. Jelinek* and *K. L. Komarek*, Mh. Chem. **105**, 917 (1974).
[4] *H. Jelinek* and *K. L. Komarek*, Mh. Chem. **105**, 689 (1974).
[5] *H. Ipser, K. L. Komarek*, and *H. Mikler*, Mh. Chem. **105**, 1322 (1974).
[6] *C. Fabre*, Ann. chim. phys. **14**, 110 (1888).
[7] *D. D. Wagman, W. H. Evans, V. B. Parker, I. Halow, S. M. Pailey*, and *R. H. Schumm*, Selected Values of Chemical Thermodynamic Properties. Techn. Note 270—4 (1969), Natl. Bur. Standards, Washington, D.C.
[8] *E. F. Westrum, Jr., C. Chou*, and *F. Grønvold*, J. Chem. Phys. **30**, 761 (1959).
[9] *J. Mikler, H. Ipser*, and *K. L. Komarek*, Mh. Chem. **105**, 977 (1974).
[10] *Yu. V. Rumyantsev, G. M. Zhiteneva*, and *F. M. Bolondz*, Tr. Vost.-Sibirsk Filiala, Akad. Nauk SSSR **41**, 114 (1962); Chem. Abstr. **58**, 4141 h (1963).
[11] *V. A. Geiderikh, Ya. I. Gerasimov*, and *A. V. Nikolskaya*, Dokl. Akad. Nauk SSSR **137**, 1399 (1961); Engl. Transl.: Proc. Acad. Sci. USSR, Phys. Chem. Sect. **137**, 349 (1961).

[12] *Ya. I. Gerasimov, A. V. Nikolskaya, V. A. Geiderikh, A. S. Abbasov,* and *R. A. Vecher*, Khim. Svyas v Poluprov, Akad. Nauk Bjelorusk SSR, Minsk 113 (1965); Engl. Transl.: Chemical Bonds in Semiconductors and Solids (*N. N. Sirota*, ed.), p. 87. New York: Consultant Bur. 1967.
[13] *K. C. Mills*, Thermodynamic Data for Inorganic Sulphides, Selenides and Tellurides. London: Butterworths. 1974.
[14] *L. S. Brooks*, J. Amer. Chem. Soc. **74**, 227 (1952).
[15] *F. Grønvold, H. Haraldsen,* and *J. Vihovde*, Acta Chem. Scand. **8**, 1927 (1954).
[16] *R. Hultgren, P. D. Desai, D. T. Hawkins, M. Gleiser, K. K. Kelley,* and *D. D. Wagman*, Selected Values of the Thermodynamic Properties of the Elements. Metals Park, Ohio: ASM. 1973.

Prof. Dr. K. L. Komarek
Institute of Inorganic Chemistry
University of Vienna
Währinger Straße 42
A-1090 Wien
Austria